



OPEN ACCESS

EDITED BY

Kin Fai (Kenneth) Tong,
Hong Kong Metropolitan University, Hong Kong
SAR, China

REVIEWED BY

Luciano Miuccio,
University of Catania, Italy
Ahmad Bazzi,
New York University Abu Dhabi, United Arab
Emirates

*CORRESPONDENCE

Leila Tlebaldiyeva,
✉ ltlebaldiyeva@nu.edu.kz

RECEIVED 29 November 2025

REVISED 07 January 2026

ACCEPTED 12 January 2026

PUBLISHED 17 February 2026

CITATION

Tlebaldiyeva L, Naurzybayev G, Dairanbek A and
Arzykulov S (2026) Fairness optimization in RIS-
FAS NOMA networks under
practical impairments.
Front. Commun. Netw. 7:1756675.
doi: 10.3389/frcmn.2026.1756675

COPYRIGHT

© 2026 Tlebaldiyeva, Naurzybayev, Dairanbek
and Arzykulov. This is an open-access article
distributed under the terms of the [Creative
Commons Attribution License \(CC BY\)](#). The use,
distribution or reproduction in other forums is
permitted, provided the original author(s) and
the copyright owner(s) are credited and that the
original publication in this journal is cited, in
accordance with accepted academic practice.
No use, distribution or reproduction is permitted
which does not comply with these terms.

Fairness optimization in RIS-FAS NOMA networks under practical impairments

Leila Tlebaldiyeva*, Galymzhan Naurzybayev, Aigerim Dairanbek
and Sultangali Arzykulov

Department of Electrical and Computer Engineering, School of Engineering and Digital Sciences,
Nazarbayev University, Astana, Kazakhstan

For future wireless networks beyond 5G (B5G), integrating and dynamically reconfiguring advanced technologies is crucial for achieving high spectral efficiency and ensuring massive user connectivity. This work proposes a practical and improved millimeter-wave non-orthogonal multiple access (NOMA) framework that synergistically integrates a reconfigurable intelligent surface (RIS) with fluid antenna system (FAS) receivers. The port selection diversity of FAS is utilized to enhance signal reception and aid interference suppression during successive interference cancellation (SIC). A central contribution is the development of a max-min fairness-based power allocation (PA) algorithm designed to equalize the ergodic capacities of NOMA users by maximizing the minimum achievable signal-to-interference-plus-noise ratio (SINR) under imperfect SIC conditions, ensuring a fair and balanced rate distribution. Crucially, three major practical impairment sources, such as the combined impact of channel state information (CSI) with bounded estimation error, finite-resolution RIS phase-shift quantization, and residual interference due to imperfect SIC with configurable error levels are explicitly modeled and analyzed. Simulation results evaluate the system performance across various transmit power and FAS port numbers, conclusively demonstrating that the RIS-FAS integration yields substantial gains in ergodic capacity, successfully balances spectral efficiency with user fairness, and highlights the critical trade-offs necessary for realistic networks.

KEYWORDS

ergodic capacity, fairness optimization, FAS, NOMA, RIS, practical impairments

1 Introduction

As the number of connected devices in future communication systems increases exponentially, the demand for fast and reliable wireless services becomes critical. It is projected that the number of connected IoT devices will almost double from 20.1 billion devices in 2025 to 39.6 billion in 2033 (Statista Research Department, 2023). The rapid growth of connected devices has raised interest in exploring advanced communication systems that enhance spectral utilization and adapt to complex propagation environments. Wireless technologies such as reconfigurable intelligent surfaces (RISs) (Shaikh et al., 2022; Rostami Ghadi et al., 2024), non-orthogonal multiple access (NOMA) (Tlebaldiyeva et al., 2021), and fluid antenna systems (FASs) have each independently demonstrated significant potential to improve system performance through intelligent channel shaping, spectrum efficiency, and spatial diversity (Tlebaldiyeva et al., 2024; Tlebaldiyeva et al., 2023). Integrating these technologies offers new degrees of freedom to improve fundamental

performance metrics, especially ergodic capacity, which quantifies the long-term average achievable rate under fading channels.

RIS has gathered interest for its ability to passively shape the wireless environment via programmable phase shifts that improve base station (BS)-to-user channel propagation (Trigui et al., 2020). It offers high spectral and energy efficiency with numerous reflective elements, making it a key beyond the 5G (B5G) enabler (Hu et al., 2018).

In addition, the recent research in (Bazzi and Chafii, 2025) presented a RIS-assisted network to enhance passive radar target localization by using the RIS to establish robust links to redirect weak, target-reflected communication signals towards the radar, effectively turning communication infrastructure into a sensing asset by jointly optimizing the sensing and communication technology. Nevertheless, providing effective support for numerous users with simultaneous access is still an open challenge. One of the multiple access techniques, NOMA, differentiates itself from other traditional methods, such as time, frequency, or code multiplexing, by allowing users to simultaneously utilize the same time-frequency resource block, thus enhancing spectrum efficiency and ensuring user fairness (Huang et al., 2018). Combining the advantages of RIS and NOMA have been investigated in a number of papers since both methods are very promising. Prior research in (Vu et al., 2024a; Shaikh et al., 2022) showed that, when used in conjunction with power domain multiplexing strategies like NOMA, RIS can greatly boost system capacity and produce high data transmission rates in fading environments. Realistic fading and hardware limitations must be taken into consideration for the practical assessment of RIS-assisted millimeter-wave (mmWave) NOMA networks. In urban and indoor mmWave environments, Nakagami- m fading accurately models both LOS and non-LOS (NLOS) conditions (Awad and Abdel-Hafez, 2025). FAS improves resilience in RIS-NOMA networks by increasing reconfigurability with respect to shape, bandwidth, frequency, and spatial diversity (Rostami Ghadi et al., 2024). Electromagnetic reconfigurable FAS prototypes have shown an improved received power and a bit error rate over conventional arrays, using software-controlled fluids for dynamic radiation, increasing spectral efficiency and adaptability (Wang et al., 2025). Liquid metal materials enable flexible, compact antenna designs suitable for dynamic environments (Wang M. et al., 2022). Closed-form expressions for FAS outage probability and diversity gain under Jake's model were derived in (New et al., 2024), proposing a suboptimal FAS design with port estimation. Spatial selection allows FAS to adapt to favorable signals, helping mitigate fading in RIS-influenced environments. Studies (Yao et al., 2026) and (Yao et al., 2025) confirm RIS-FAS integration improves capacity under spatial correlation, yet analytical models jointly addressing RIS-assisted NOMA with fairness power control, correlated Nakagami- m fading remain scarce.

Furthermore, most existing studies on RIS and RIS-FAS-aided NOMA assume ideal hardware and perfect channel knowledge or model all non-idealities as a single effective noise term (Li et al., 2023; Shaikh et al., 2025). In practice, there are several practical noises that jointly limit the performance of the NOMA-RIS-FAS networks (Shaikh et al., 2025; Ammisetty and Ramarakula, 2025; Vu et al., 2024b). First, the acquisition of perfect channel state information (CSI) remains impossible because mmWave frequencies require element-wise CSI estimation, which becomes infeasible due to pilot overhead and feedback constraints (Li et al., 2023; Ammisetty and Ramarakula, 2025). It was established that estimation errors translate into channel-mismatch during

beamforming (Li et al., 2023), NOMA power-domain user ordering (Ammisetty and Ramarakula, 2025), and degrade both capacity and fairness. Second, imperfect successive interference cancellation (SIC) leaves a non-negligible fraction of intra-cluster interference at strong users, due to channel uncertainty, decoding errors, or hardware limitations (Pandey and Bansal, 2023; Vu et al., 2024b). Especially, this residual interference becomes more pronounced when users are closely spaced in power or experience spatial correlation (Wang T. et al., 2022; Aldababsa et al., 2022). Last, the signal-dependent distortion from hardware impairments and quantization effects restricts data transfer rates when the signal-to-noise ratio reaches high levels (Qian et al., 2020). The effective diversity order decreases because of correlated fading between the RIS elements and FAS ports, which makes these imperfections more severe for user fairness. The current research lacks models that analyze RIS-assisted NOMA systems with FAS under Nakagami- m fading while separately handling CSI errors, SIC residuals impairments, and phase noise quantization distortions. This gap motivates a fairness-oriented analysis of RIS-FAS-NOMA networks under practical noise conditions.

According to Monte Carlo simulation results, the proposed RIS-FAS-NOMA configuration was found to significantly increase achievable data rates while maintaining fairness, particularly for disadvantaged users, even under practical impairments. It can be observed that the increase in the number of FAS ports and RIS elements leads to an improvement in performance, thereby emphasizing the benefits of co-optimized reconfigurable systems. The simulation results confirm that higher transmit power and more RIS/FAS components enhance ergodic capacity but expose fairness issues among NOMA users. User proximity to RIS, imperfect CSI, RIS phase-shift quantization errors, and residual interference from imperfect SIC substantially impact system performance. Fairness-based PA, combined with sufficient FAS ports and well-optimized RIS elements, can mitigate these issues to some extent, although practical imperfections remain a critical bottleneck. These findings underscore the importance of balanced design in achieving both high throughput and equitable user experiences in B5G networks.

The main contributions of this work are highlighted below:

- A practical and improved mmWave NOMA network is proposed, integrating FAS-receivers and RIS, where port selection diversity of FAS enhances signal reception and aids interference suppression during SIC.
- A max-min fairness-based PA algorithm is developed to equalize the ergodic capacities of NOMA users. The algorithm maximizes the minimum achievable signal-to-interference-plus-noise ratio (SINR) under imperfect SIC conditions, ensuring a fair and balanced rate distribution.
- Three major practical impairment sources are explicitly modeled and analyzed: CSI with bounded estimation error, finite-resolution RIS phase-shift quantization, and residual interference due to imperfect SIC with configurable error levels.
- Simulation results are presented to evaluate the proposed system performance. Ergodic capacity metrics are analyzed with respect to transmit power and the number of antenna elements, illustrating trade-offs between spectral efficiency, fairness, and RIS/FAS configurations.

The paper is structured as follows. Section II details the system model, followed by the channel model and fairness-based power allocation in Sections III and IV. Finally, numerical results and conclusions are presented in Sections V and VI.

We use the following notation in the paper: $\mathbb{E}(\cdot)$ stands for the expectation operator, $J_0(\cdot)$ denotes zero-order Bessel function of the first kind and $\mathcal{N}(a, c)$ is the Gaussian random variable (RV) with mean a and variance c .

2 System model

We study an RIS-assisted NOMA network with two users as shown in Figure 1. It is assumed that a base station (S) is equipped with a single antenna and that far- and near-located users (u_1 and u_2) are assisted with L -port FAS receivers. The practical application of NOMA is typically restricted to two-user clusters, as the computational complexity of SIC scales non-linearly with the number of active devices. Expanding the cluster size beyond $N = 2$ introduces significant drawbacks, including elevated processing latency and increased power consumption at the receiver (Tlebaldiyeva et al., 2021). We consider that there is no direct link between S and users due to the blockage. The N -element RIS is divided into two subarrays, N_1 and N_2 , to establish alternative links to u_1 and u_2 . RIS creates an optimal phase shift to focus the distant signals. Within the NOMA framework, power is allocated using PA coefficients that ensure fairness among users. Moreover, both users are equipped with FAS-aided receivers that can select the best channel among multiple antenna ports.

We assume ideal channel state information for the S -to-RIS link, as the locations of S and RIS are known and can be estimated through the evaluation of the angle of arrival and departure. However, the RIS-to-users link is imperfect due to channel estimation error and limited feedback. Moreover, we investigate the impact of quantization phase errors originating from RIS.

3 Channel and signal model

3.1 BS-to-RIS channel

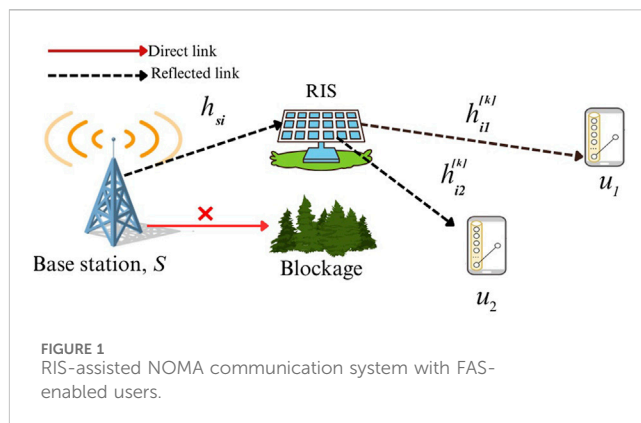
The channel between the BS and the i -th RIS element follows an independent and identically distributed Nakagami- m fading, which is commonly used to model wireless channels for both LOS/NLOS channel components as

$$h_{si} \sim \text{Nakagami} - m(m, \Omega), \forall i \in \{1, N\}, \quad (1)$$

where m is the fading parameter, which determines the severity of fading, and Ω is the power parameter, representing the average received power of the channel.

3.2 RIS-to-user channels

The i -th RIS element-to-user channel port k follows a correlated Nakagami- m fading distribution. Similar to (Tlebaldiyeva et al., 2022),



the spatially correlated Nakagami- m channel at port k is defined as $h_{iq}^{[k]} = \sum_{l=1}^m |\sqrt{(1-r)}x_{il} + \sqrt{r}x_{0l} + j(\sqrt{(1-r)}y_{il} + \sqrt{r}y_{0l})|^2$, where $\forall k \in \{1, L\}, q \in \{1, 2\}$, x_{il} , x_{0l} , y_{il} , and y_{0l} are independent Gaussian RVs, with zero mean and 1/2 variance. As each user is equipped with an FAS receiver, a spatial correlation among the L reception ports is employed. This correlation is determined using the land-mobile correlation model as in (Wong et al., 2022)

$$r = \left| \frac{2}{L(L-1)} \sum_{k=1}^{L-1} (L-k) J_0 \left(\frac{2\pi kW}{L-1} \right) \right|, \quad (2)$$

where r is the correlation coefficient and W is the antenna coefficient size. Since a FAS operates by shifting a single port across L discrete ports within a linear $W \times \lambda$ antenna size, where λ is the operational wavelength, the zero-order Bessel function is used to quantify how the channel gain at one port relates to another. When the argument of $J_0(x)$ is small, and ports are densely located, the correlation is near 1, meaning the ports experience a similar channel. As the distance increases, the value of $J_0(x)$ drops, representing the spatial diversity that FAS exploits to find a stronger signal. We have applied a spatial correlation model for our system model from (Wong et al., 2022).

3.3 Imperfect channel state information model

The imperfect channel from RIS element i to a user $q, q \in \{1, 2\}$, is modeled as

$$h_{iq}^{[k]} = \rho \hat{h}_{iq}^{[k]} + \sqrt{1-\rho^2} \Delta h_{iq}^{[k]}, \quad (3)$$

where $q \in \{1, 2\}$, $\hat{h}_{iq}^{[k]}$ is an estimated channel (known at the receiver), $\Delta h_{iq}^{[k]}$ is channel estimation error modelled as Gaussian RV with zero mean and σ^2 variance, ρ is correlation coefficient between actual and estimated channels ($0 \leq \rho \leq 1$).

3.4 Effective received signals with imperfect CSI and phase noise at port k for both users

The received signal at the port k of the further located u_1 is given as

$$y_1^{[k]} = \underbrace{\sqrt{\frac{P}{d_{sr}^\tau d_{r1}^\tau} \rho \sum_{i=1}^{N_1} h_{si} \hat{h}_{i1}^{[k]} e^{j\delta_i} \chi}}_{\text{desired signal}} + \underbrace{\sqrt{\frac{P}{d_{sr}^\tau d_{r1}^\tau} \sqrt{1-\rho^2} \sum_{i=1}^{N_1} h_{si} \Delta h_{i1}^{[k]} e^{j\delta_i} \chi + \eta_k}}_{\text{interference due to imperfect CSI}} \quad (4)$$

$$f_{\delta_i}(\delta) = \begin{cases} \frac{Q}{2\pi}, & -\frac{\pi}{Q} \leq \delta \leq \frac{\pi}{Q} \\ 0, & \text{otherwise,} \end{cases} \quad (6)$$

where $\chi = \sqrt{\alpha_1} s_1 + \sqrt{\alpha_2} s_2$ is transmitted signal with $\mathbb{E}[|s_q|^2] = 1$. Similarly, the received signal at user 2 of the port k is given as

$$y_2^{[k]} = \underbrace{\sqrt{\frac{P}{d_{sr}^\tau d_{r2}^\tau} \rho \sum_{i=1}^{N_2} h_{si} \hat{h}_{i2}^{[k]} e^{j\delta_i} \chi}}_{\text{desired signal}} + \underbrace{\sqrt{\frac{P}{d_{sr}^\tau d_{r2}^\tau} \sqrt{1-\rho^2} \sum_{i=1}^{N_2} h_{si} \Delta h_{i2}^{[k]} e^{j\delta_i} \chi + \eta_k}}_{\text{interference due to imperfect CSI}} \quad (5)$$

where h_{si} is the channel from S to RIS element i , $\delta_i = \phi_i + \psi_i - \beta_i$ is a residual phase error due to quantization, ϕ_i and ψ_i are channel phases from S -to-RIS and RIS-to-user and β_i is an actual phase shift applied by RIS element i , η_k is an additive Gaussian noise with a zero mean and variance σ_k^2 , d_{sr} , d_{r1} are distances for S -to-RIS and RIS-to-user links, and τ is a path loss exponent of the channel.

Require: Channel parameters: $h_{si}, \hat{h}_{iq}^{[k]}, \Delta h_{in}^{[k]}$; SIC error: ε ; Noise: σ_q^2 ; Transmit power settings: $P_{\min}, P_{\max}, \Delta P$; Iterations: T ;
Ensure: Optimal average PA factors: $\bar{\alpha}_1, \bar{\alpha}_2$; Average capacities: \bar{C}_1, \bar{C}_2 ;
Initialize: Empty lists $\mathcal{A}_1, \mathcal{A}_2, \mathcal{C}_1, \mathcal{C}_2$;
for $P = P_{\min}$ **to** P_{\max} **step** ΔP **do**
 for $iter = 1$ **to** T **do**
 Generate random channel realizations h_{si} and $\hat{h}_{iq}^{[k]}$
 for all ports $k \in L$; $A_1 \leftarrow \rho^2 \cdot \max_{k \in L} |\sum_{i=1}^{N_1} h_{si} \hat{h}_{i1}^{[k]} e^{j\delta_i}|^2$;
 $A_2 \leftarrow \rho^2 \cdot \max_{k \in L} |\sum_{i=1}^{N_2} h_{si} \hat{h}_{i2}^{[k]} e^{j\delta_i}|^2$;
 $B_1 \leftarrow (1-\rho^2) |\sum_i h_{si} \Delta h_{i1}^{[k]} e^{j\delta_i}|^2 + \frac{\sigma_1^2}{\bar{P}^2}$;
 $B_2 \leftarrow (1-\rho^2) |\sum_i h_{si} \Delta h_{i2}^{[k]} e^{j\delta_i}|^2 + \frac{\sigma_2^2}{\bar{P}^2}$;
 $a \leftarrow A_1 A_2$; $b \leftarrow A_1 (B_2 + \varepsilon) + A_2 B_1$; $c \leftarrow -A_1 (B_2 + \varepsilon)$;
 $\alpha_2 \leftarrow \frac{-b + \sqrt{b^2 - 4ac}}{2a}$; $\alpha_1 \leftarrow 1 - \alpha_2$;
 $\gamma_1 \leftarrow \frac{\alpha_1 A_1}{B_1 + \alpha_2 A_1}$; $\gamma_2 \leftarrow \frac{\alpha_2 A_2}{B_2 + \varepsilon}$;
 $C_1 \leftarrow \log_2(1 + \gamma_1)$; $C_2 \leftarrow \log_2(1 + \gamma_2)$; Append results to $\mathcal{A}_1, \mathcal{A}_2, \mathcal{C}_1, \mathcal{C}_2$;
 Return $\text{mean}(\mathcal{A}_q), \text{mean}(\mathcal{C}_q)$ for $q \in \{1, 2\}$

Algorithm 1. Fairness-Driven NOMA Power Allocation with FAS Port Selection.

3.5 Phase error distribution due to quantization

RIS cannot generate all desired phases and, in practice, can create a limited number of phases towards the users, which is denoted by Q^b , where b is the number of quantization bits. Inspired by (Zhakipov et al., 2023), the phase errors are modeled as a uniform distribution with the following probability density function

where $Q = 2^b$ is the number of discrete phase shifts and b stands for the number of quantization bits.

3.6 Signal-to-interference-plus-noise ratio (SINR)

For the far user, u_1 , the goal is to decode its own signal s_1 while treating the near user's signal, s_2 , as interference. The SINR at u_1 at the given port k is formulated as

$$\gamma_1^{[k]} = \frac{\alpha_1 \rho^2 \left| \sum_{i=1}^{N_1} h_{si} \hat{h}_{i1}^{[k]} e^{j\delta_i} \right|^2}{(1-\rho^2)\xi + \alpha_2 \rho^2 \left| \sum_{i=1}^{N_1} h_{si} \hat{h}_{i1}^{[k]} e^{j\delta_i} \right|^2 + \frac{\sigma_1^2}{\bar{P}^2}} \quad (7)$$

where $\bar{P} = \sqrt{\frac{P}{d_{sr}^\tau d_{r1}^\tau}}$ and $\xi = |\sum_{i=1}^{N_1} h_{si} \Delta h_{i1}^{[k]} e^{j\delta_i}|^2$. Since u_1 is the far user, it does not perform SIC and must treat u_2 signal as noise. The FAS output at u_1 is evaluated as $\gamma_1 = \max_{k \in L} (\gamma_1^{[k]})$.

Near user u_2 performs SIC by first decoding u_1 's signal and subtracting it, and then decoding its own signal. Thus, the SINR for u_2 at port k is given as

$$\gamma_2^{[k]} = \frac{\alpha_2 \rho^2 \left| \sum_{i=1}^{N_2} h_{si} \hat{h}_{i2}^{[k]} e^{j\delta_i} \right|^2}{(1-\rho^2) \left| \sum_{i=1}^{N_2} h_{si} \Delta h_{i2}^{[k]} e^{j\delta_i} \right|^2 + \varepsilon + \frac{\sigma_2^2}{\bar{P}^2}} \quad (8)$$

where $\varepsilon = \varepsilon \alpha_1 \rho^2 \left| \sum_{i=1}^{N_1} h_{si} \hat{h}_{i2}^{[k]} e^{j\delta_i} \right|^2$ stands for the imperfect SIC term of u_1 that u_2 failed to cancel perfectly and ε is the SIC error coefficient, $0 \leq \varepsilon \leq 1$. Next, the FAS output for u_2 is given as $\gamma_2 = \max_{k \in L} (\gamma_2^{[k]})$.

4 Fairness-based power allocation

In this section, we propose a max-min fairness-driven PA strategy to equalize the ergodic capacities of the two NOMA users in the presence of practical impairments, i.e., imperfect CSI, finite-resolution RIS phase shifts, and residual interference due to imperfect SIC. Since the ergodic capacity is a monotonically increasing function of the SINR, maximizing the minimum ergodic capacity across users is equivalent to maximizing the minimum SINR. To achieve max-min fairness, we set $\gamma_1 = \gamma_2$. We define the effective channel power terms in terms of A_q and B_q , $q \in \{1, 2\}$, coefficients as follows

$$A_q = \bar{P} \cdot \max_k \left(\rho^2 \left| \sum_{i=1}^{N_q} h_{si} \hat{h}_{in}^{[k]} e^{j\delta_i} \right|^2 \right), \quad (9)$$

$$B_q = (1-\rho^2) \left| \sum_{i=1}^{N_q} h_{si} \Delta h_{iq}^{[k]} e^{j\delta_i} \right|^2 + \frac{\sigma_k^2}{\bar{P}^2}. \quad (10)$$

Solving the quadratic equation $\alpha a^2 + b \alpha + c = 0$ yields the optimal factor α_q^* with the following parameters

- $a = A_1 A_2$,
- $b = A_1 (B_2 + \varepsilon) + A_2 B_1$,
- $c = -A_1 (B_2 + \varepsilon)$.

The optimal power allocation is $\alpha_2^* = \frac{-b + \sqrt{b^2 - 4ac}}{2a}$ and $\alpha_1^* = 1 - \alpha_2^*$.

5 Computational complexity analysis

The computational complexity of the proposed Fairness-based NOMA-FAS algorithm is primarily determined by the system parameters, such as the RIS elements and FAS ports. For a given transmit power P , the complexity analysis is as follows. Generating the channels for N RIS elements across L FAS ports for two users requires $\mathcal{O}(T \cdot L \cdot N)$ operations. The maximization process to find A_q and B_q involves computing the magnitude of the RIS-summation for each port, which scales as $\mathcal{O}(T \cdot L \cdot N)$. The calculation of coefficients a, b, c and the subsequent quadratic formula to find α_2^* requires only basic arithmetic operations, resulting in a complexity of $\mathcal{O}(T)$. Therefore, the total computational complexity of Algorithm 1 is given by

$$C_{total} = \mathcal{O}(T \cdot L \cdot N). \quad (11)$$

6 Ergodic capacity

The performance metric of primary interest is the ergodic capacity of each user, defined as

$$C_q = \mathbb{E}[\log_2(1 + \gamma_q)], \quad q = 1, 2, \quad (12)$$

where the expectation is taken over the random channel realizations, estimation errors $\Delta h_{iq}^{[k]}$, phase quantization errors δ_i , and FAS port selection.

Because of the max-operation over L correlated Nakagami- m ports, the presence of bounded CSI error $\rho < 1$, finite-resolution phase shifts, and residual SIC interference ϵ , a closed-form expression for C_q is mathematically intractable. Therefore, we evaluate the ergodic capacity numerically using Monte Carlo simulation with $T = 10^6$ independent channel realizations

$$\hat{C}_q = \frac{1}{T} \sum_{t=1}^T \log_2(1 + \gamma_q^{(t)}), \quad q = 1, 2, \quad (13)$$

where \hat{C}_q is an average ergodic capacity, $\gamma_q^{(t)}$ is the SINR of user q in the t -th realization after optimal port selection at the FAS receiver and fairness-driven PA.

The normalized ergodic sum capacity is computed as

$$C_{sum} = \frac{\hat{C}_1 + \hat{C}_2}{\log_2(1 + \bar{P}/\sigma^2)} \quad (14)$$

to fairly compare different transmit power levels and impairment scenarios.

7 Numerical results

In this section, we will investigate how the practical system noises affect the normalized ergodic capacity of the proposed system model. We discuss findings via Monte Carlo simulations run for 10^6 iterations per data point. The default system parameters for these simulations are listed in Table 1. We assume the same number of RIS

TABLE 1 Simulation parameters and values.

Parameter	Description	Value
L	Number of FAS ports	{0 ... 100}
m	Fading parameters	{2, 3, 4}
P	Transmit power	{-10, ..., 29} dBm
N_q	Number of reflecting elements	{20, 50, 100}
τ	PLE	{2, 3, 4}
d_{sr}	A distance from the BS to RIS	50 m
d_{r1}	A distance from RIS to u_1	150 m
d_{r2}	A distance from RIS to u_2	100 m
Q	Number of quantization bits	{1, 3, ∞ }
W	Antenna size coefficient	{0.5, 1, 2}
ρ	CSI correlation coefficient	{0.7, 0.8, 0.9, 1}

elements dedicated to each user, $N_1 = N_2$. In this work, we focus on a max-min fairness-based (MMF) PA scheme designed to ensure equitable resource distribution among users. Although this approach yields a lower ergodic sum-rate compared to sum-rate maximization (SRM) strategies, given in Figure 2, it significantly improves Jain's fairness index as shown in Figure 3.

Figure 2 depicts the normalized ergodic capacity as a function of the number of RIS ports for different $P = \{0, 10\}$ dBm and $W = \{0.5, 1, 2\}$ parameters given $\epsilon = 0$. A consistent performance gap is observed between the SRM and MMF strategies across all simulated scenarios. The SRM algorithm consistently yields a higher total ergodic capacity than the MMF algorithm. For instance, at $L = 60$ with $P = 10$ dBm and $W = 2$, the SRM scheme achieves approximately 9.75 bits/s/Hz, while the MMF scheme reaches roughly 9.55 bits/s/Hz. This gap quantifies the cost of fairness: the SRM algorithm opportunistically allocates more resources to the user with the stronger channel to maximize the sum, whereas the MMF algorithm sacrifices total throughput to boost the weaker user's rate, resulting in a lower aggregate capacity. Moreover, both algorithms exhibit a logarithmic growth in capacity as the number of RIS ports increases from 10 to 60. This confirms that increasing the number of RIS elements enhances the array gain and passive beamforming capability.

Figure 3 illustrates the impact of the number of RIS elements on the system's fairness, quantified using Jain's fairness index, for different W and transmit power. The figure compares the performance of the proposed MMF-based algorithm against the benchmark SRM scheme. As observed from the constant horizontal line at the top of the graph, the MMF-based power allocation strategy achieves a Jain's index of 1.0 across all simulated scenarios, regardless of the values of N , $W = \{0.5, 1, 2\}$, and $P = \{0, 10\}$ dBm. This confirms the effectiveness of the MMF formulation, which is explicitly designed to maximize the minimum user rate. In contrast, the SRM algorithm, which prioritizes total system capacity, exhibits a significantly lower fairness index, ranging from approximately 0.62–0.74. This disparity arises because the SRM objective inherently favors users with stronger channel conditions to maximize the arithmetic sum of rates, often allocating disproportionately lower power to users with weaker channels

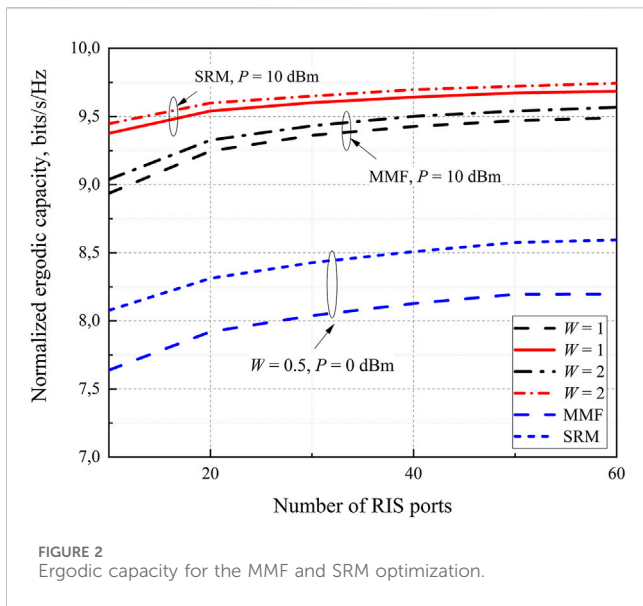


FIGURE 2 Ergodic capacity for the MMF and SRM optimization.

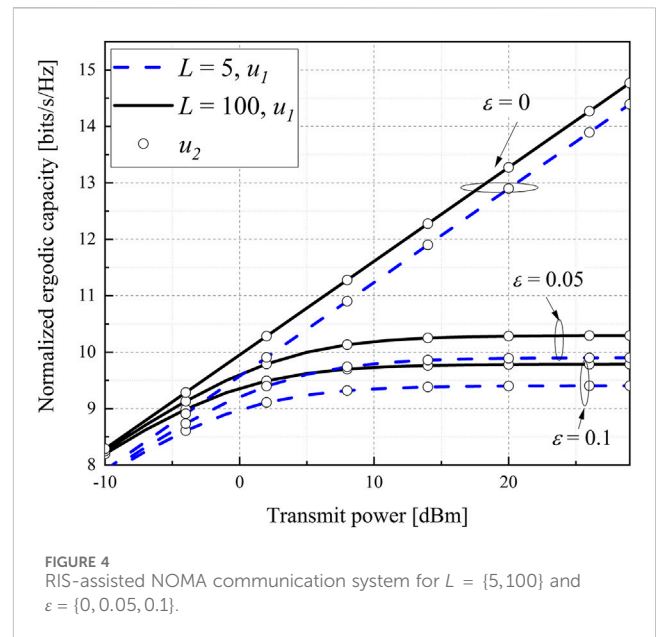


FIGURE 4 RIS-assisted NOMA communication system for $L = \{5, 100\}$ and $\epsilon = \{0, 0.05, 0.1\}$.

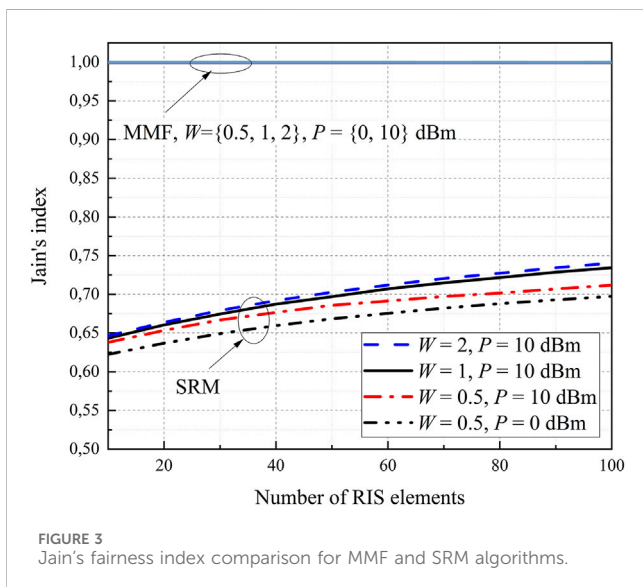


FIGURE 3 Jain's fairness index comparison for MMF and SRM algorithms.

Figure 4 illustrates the complex interplay between transmit power, number of FAS ports, and SIC error on the system's performance. A primary observation is the significant capacity degradation caused by the non-ideal SIC, where increasing the SIC error, ϵ , from 0 (ideal) to 0.1 drastically lowers the capacity floor, indicating the system rapidly becomes noise-limited. For $\epsilon > 0$, the capacity quickly reaches a saturation point above 10 dBm transmit power, demonstrating that simply increasing power offers no further gain once nonlinear noise sources dominate the link budget. The performance difference between $L = 5$ and $L = 100$ FAS ports is substantial, confirming that increasing the receiver diversity gain effectively mitigates the system's noise limitations. Specifically, the large $L = 100$ array not only provides higher peak capacity but also delays the onset of saturation compared to the $L = 5$ configuration across all noise levels. The capacities of both users, u_1 and u_2 , maintain nearly identical values throughout all scenarios, suggesting that the fairness algorithm has successfully

ensured equitable access and performance for both NOMA users. Overall, this figure shows that maximizing receiver diversity is a more effective strategy for improving capacity in the presence of SIC than relying solely on increased transmission power.

Figure 5 illustrates the relationship between the normalized ergodic capacity and the number of FAS ports in a system for different numbers of RIS elements $N_1 = N_2 = \{5, 20\}$ and imperfect SIC noises $\epsilon = \{0, 0.05, 0.1\}$. There is a clear, positive correlation between the number of RIS, antenna ports, and the system's capacity. As the number of ports increases, the normalized ergodic capacity also slightly increases. The curve $\epsilon = 0$ represents the ideal case with no SIC error that serves as the upper performance bound. The SIC noise has a detrimental effect on the system performance. For example, the ergodic performance degrades to 49.7% from ideal SIC to $\epsilon = 0.1$ case at $L = 100$. A critical observation is the saturation of gains. While capacity initially rises steeply with the number of ports, the rate of increase slows down. Moreover, N_1 and N_2 are the primary factors determining the passive beamforming gain provided by the RIS. As N_1 and N_2 increase from 20 to 100, the system exhibits a substantial capacity shift due to the multiplicative growth, resulting in a higher normalized ergodic capacity floor across all plots. For example, in ideal SIC plots of $L = 100$ and $L = 20$, the ergodic capacities are recorded as 14.94 bits/s/Hz and 12.62 bits/s/Hz, contributing to the difference in performance 15.47%.

Figure 6 illustrates the critical influence of the CSI correlation coefficient ρ on the system's normalized ergodic capacity across varying numbers of FAS ports. The correlation ρ is the dominant factor determining the capacity ceiling: a small reduction from $\rho = 1.0$ (perfect CSI) to $\rho = 0.7$ results in an immense capacity loss, dropping the capacity from over 11 bits/s/Hz to just above 6 bits/s/Hz. While increasing the number of FAS ports provides a small initial boost in capacity, the performance curves for all ρ values quickly flatten out around $L = 40$. The capacity separation between the different ρ curves remains constant for high L , confirming that the system is ultimately limited by the self-interference term $\sqrt{1 - \rho^2} \Delta h_{id}^{[k]}$ due to inaccurate channel estimation.

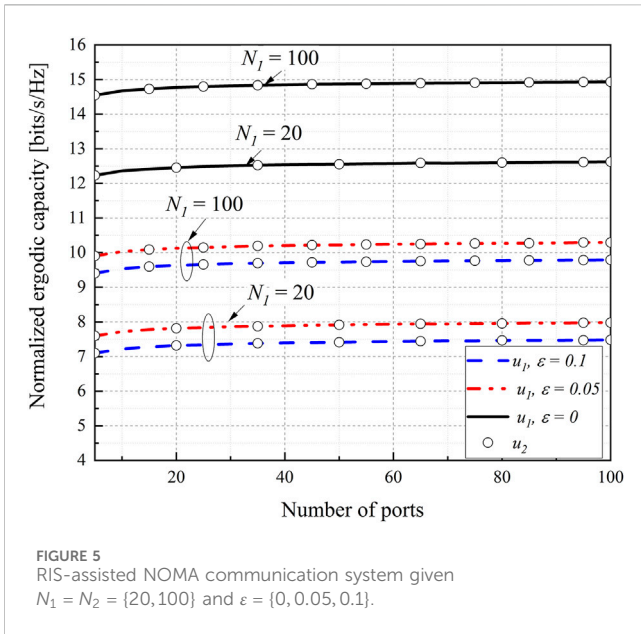


FIGURE 5 RIS-assisted NOMA communication system given $N_1 = N_2 = \{20, 100\}$ and $\epsilon = \{0, 0.05, 0.1\}$.

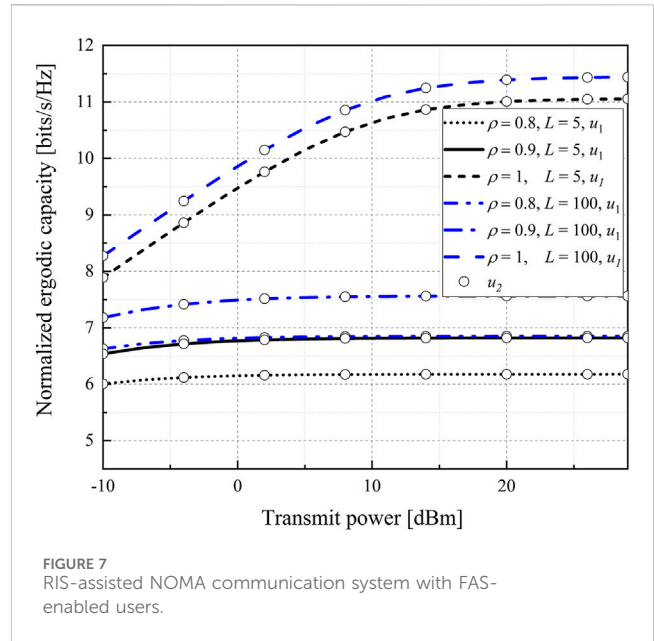


FIGURE 7 RIS-assisted NOMA communication system with FAS-enabled users.

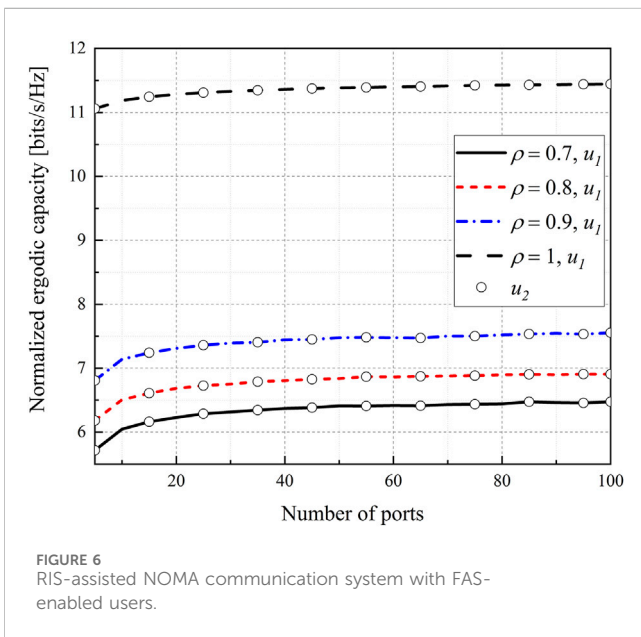


FIGURE 6 RIS-assisted NOMA communication system with FAS-enabled users.

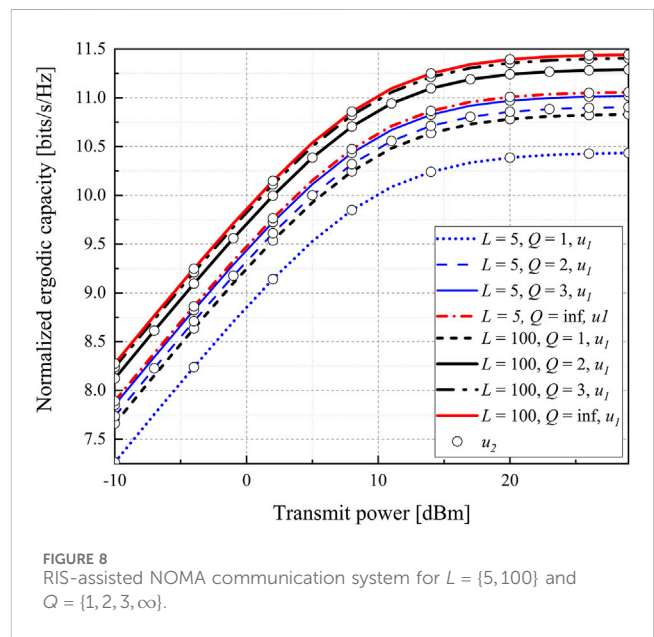


FIGURE 8 RIS-assisted NOMA communication system for $L = \{5, 100\}$ and $Q = \{1, 2, 3, \infty\}$.

Similarly, Figure 7 demonstrates the joint impact of ρ and the number of FAS ports on the system’s normalized ergodic capacity as a function of transmit power. There is a slight performance gap achieved by increasing the number of ports from $L = 5$ to $L = 100$: for perfect CSI, the $L = 100$ configuration provides a gain of approximately 0.5 bits/s/Hz over $L = 5$ at 29 dBm. While ideal CSI curves increase with transmit power due to higher received signal strength, the plots with non-ideal CSI experience premature capacity saturation around 10 dBm due to imperfect CSI noise that limits the maximum achievable capacity, regardless of power and spatial diversity of FAS. For example, the capacity gap between $\rho = 1$ and $\rho = 0.8$ remains large even at $L = 100$ (around 4.65 bits/s/Hz), confirming that

improving CSI accuracy remains critical even when excellent receiver processing is available.

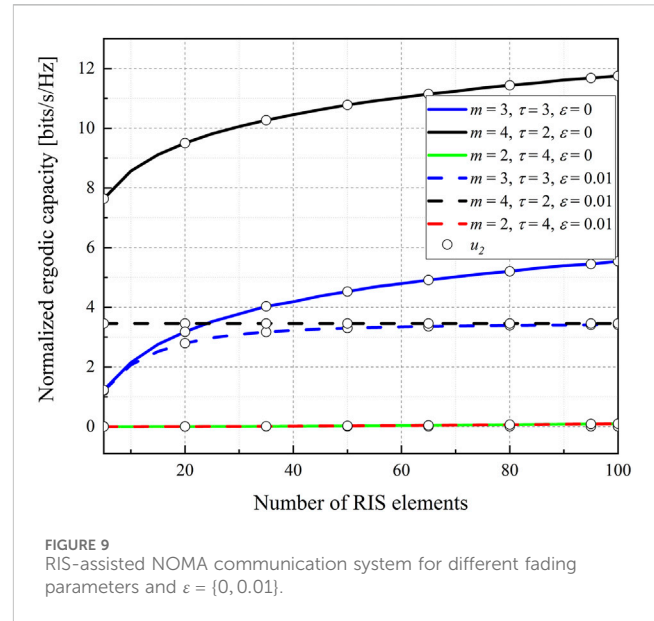
Next, Figure 8 illustrates the influence of the number of quantization bits, which is observed to impact the ergodic capacity, particularly at high transmit power. The ideal case of infinite quantization ($Q = \text{inf}$), which corresponds to zero phase error, sets the upper capacity bound for both $L = 5$ and $L = 100$ configurations. The performance penalty for reducing Q from 3 bits to 1 bit is considerable, resulting in a capacity gap (around 0.63 bits/s/Hz at 20 dBm for $L = 100$), which confirms that coarse quantization introduces a considerable phase noise limit. Increasing the number of FAS ports from $L = 5$ to $L = 100$ improves the adverse effect of phase noise. For example, at

$Q = \text{inf}$ and $P = 29$ dBm, there is 0.4 bits/s/Hz performance improvement. This suggests that FAS diversity could be used as a mitigation strategy against the phase noise caused by quantization errors.

Figure 9 investigates the combined effects of fading environment and imperfect SIC on ergodic capacity versus the number of FAS ports. The three distinct fading scenarios are clearly separated: the upper curves, corresponding to the favorable LOS channel with $m = 4, \tau = 2$, show significantly higher capacity than the lower curves, which represent the urban scenario $m = 3, \tau = 3$, and severe NLOS channel with $m = 2$ and $\tau = 4$ parameters. It is observed that physical channel parameters significantly dictate the baseline performance. Furthermore, the results reveal a fundamental bottleneck introduced by imperfect SIC. While the capacity scales logarithmically with N under perfect cancellation $\varepsilon = 0$, the presence of even minor residual interference $\varepsilon = 0.01$ causes the capacity to saturate rapidly, creating a distinct performance ceiling. This saturation phenomenon occurs because the RIS boosts the residual interference power proportionally to the desired signal, shifting the system from a noise-limited to an interference-limited regime where increasing N beyond a certain point yields diminishing returns. The NLOS scenario's capacity is nearly zero, indicating that the system is overwhelmingly dominated by the poor fading and high path loss, rendering the variations in SIC imperfection and receiver complexity negligible. Furthermore, the figure demonstrates that a higher number of RIS ports can significantly compensate for imperfect SIC. For instance, assuming $m = 3$ and $\varepsilon = 0.01$, increasing the number of elements from $N = 10$ to $N = 40$ improves the ergodic capacity from 2.08 bits/s/Hz to 3.24 bits/s/Hz. While the simulation results demonstrate significant gains in normalized ergodic capacity and fairness, the transition from theoretical models to practical hardware involves several critical constraints that must be considered. Firstly, channel estimation and CSI overhead are a main limitation for a large number of RIS elements and FAS antenna ports. As seen in (10), imperfect CSI introduces an additional noise term $(1 - \rho^2)\xi$ in the denominator, which scales with the number of RIS elements, creating a higher interference term. Secondly, estimating the channel at each antenna port location within a coherence interval is a challenging task. Practical systems may need to utilize optimization algorithms or compressed sensing to reduce the number of required pilot symbols without sacrificing diversity gains. Finally, the term ϵ in (8) represents the residual imperfect SIC noise from decoding the far user (u_1). Imperfect SIC noise scales with the power reflected by the RIS, and the system eventually enters an interference-limited regime. Moreover, numerical results indicate that the FAS-RIS integration provides the most significant capacity gains in the low-SNR regime by mitigating thermal noise through spatial diversity. Conversely, in the high-SNR regime, the system becomes interference-limited due to residual SIC, leading to a saturation of the ergodic capacity.

8 Conclusion

This paper rigorously investigated fairness-based algorithms for NOMA networks empowered by RIS-FAS technologies under



practical system noises such as imperfect CSI, hardware quantization phase errors at the RIS, and residual interference SIC. The simulation results demonstrated that poor CSI quality and severe fading at NLOS links constitute the fundamental limits on achievable capacity, often setting a hard capacity ceiling regardless of increasing transmit power or receiver diversity. A reduction in the CSI correlation coefficient from 1.0 to 0.7 resulted in a catastrophic capacity degradation of approximately 45%, confirming the vital need for high-accuracy channel estimation in RIS-enabled systems.

Crucially, the study demonstrates the efficacy of FAS diversity as a powerful mitigation strategy against these imperfections. Increasing the number of FAS ports proved highly beneficial in counteracting non-linear noise sources. For instance, $L = 100$ -port FAS significantly delayed capacity saturation in power-limited regimes and offered robust performance gains against coarse RIS quantization, $Q = 1$. Furthermore, the FAS receiver provides a measurable engineering pathway to compensate for non-ideal SIC, requiring a modest increase in ports (e.g., from $L = 5$ to $L \approx 37$) to maintain the capacity achieved under ideal SIC conditions. While the system exhibited overwhelming vulnerability to NLOS fading parameters, where capacity gains were negligible, the RIS-NOMA protocol successfully maintained excellent capacity fairness between near and far users across all simulated scenarios. Future work should focus on optimizing RIS element placement and designing robust estimation algorithms to elevate the CSI quality, thus unlocking the full potential of RIS-assisted NOMA communications.

Building upon the findings of this study, future research will extend the proposed RIS-NOMA-FAS framework to multi-cluster scenarios, where each cluster comprises two users. While the current work demonstrates that a NOMA network with two users optimizes the balance between spectral efficiency and SIC complexity, practical large-scale deployments will require sophisticated user clustering algorithms to manage a higher density of active devices.

Data availability statement

The original contributions presented in the study are included in the article/supplementary material, further inquiries can be directed to the corresponding author.

Author contributions

LT: Writing – original draft, Writing – review and editing. GN: Conceptualization, Supervision, Writing – review and editing. AD: Software, Writing – original draft. SA: Conceptualization, Formal Analysis, Funding acquisition, Investigation, Methodology, Project administration, Resources, Supervision, Writing – review and editing.

Funding

The author(s) declared that financial support was received for this work and/or its publication. This research is partially funded by the Science Committee of the Ministry of Science and Higher Education of the Republic of Kazakhstan (Grant No. AP22788920).

References

- Aldababsa, M., Khaleel, A., and Basar, E. (2022). STAR-RIS-NOMA networks: an error performance perspective. *IEEE Commun. Lett.* 26 (8), 1784–1788. doi:10.1109/lcomm.2022.3179731
- Ammisetty, M. B., and Ramarakula, M. (2025). Ergodic capacity analysis of STAR-RIS-NOMA over Nakagami- m fading channel with imperfect-CSI, inter-cell interference and SIC. *Results Eng.* 27, 106106. doi:10.1016/j.rineng.2025.106106
- Awad, S., and Abdel-Hafez, M. (2025). "RIS-NOMA systems in Nakagami- m channels: Performance metrics," in 2025 5th IEEE Middle East and North Africa Communications Conference (MENACOMM) (IEEE), 1–6.
- Bazzi, A., and Chafii, M. (2025). "Towards ISAC RIS-Enabled passive radar target localization," in ICC 2025 - IEEE International Conference on Communications, 2290–2295.
- Hu, S., Rusek, F., and Edfors, O. (2018). Beyond massive MIMO: the potential of data transmission with large intelligent surfaces. *IEEE Trans. Signal Process.* 66 (10), 2746–2758. doi:10.1109/tsp.2018.2816577
- Huang, Y., Zhang, C., Wang, J., Jing, Y., Yang, L., and You, X. (2018). Signal processing for MIMO-NOMA: present and future challenges. *IEEE Wirel. Commun.* 25 (2), 32–38. doi:10.1109/mwc.2018.1700108
- Li, Q., El-Hajjar, M., Sun, Y., Hemadeh, I., Shojaefard, A., Liu, Y., et al. (2023). Achievable rate analysis of the STAR-RIS-Aided NOMA uplink in the face of imperfect CSI and hardware impairments. *IEEE Transactions on Communications* 71 (10), 6100–6114. doi:10.1109/tcomm.2023.3287995
- New, W. K., Wong, K.-K., Xu, H., Tong, K.-F., and Chae, C.-B. (2024). Fluid antenna system: new insights on outage probability and diversity gain. *IEEE Trans. Wirel. Commun.* 23 (1), 128–140. doi:10.1109/twc.2023.3276245
- Pandey, A. K., and Bansal, A. (2023). "Coverage analysis of STAR-RIS empowered downlink NOMA with imperfect SIC," in 2023 IEEE Wireless Communications and Networking Conference (WCNC), 1–6.
- Qian, X., di Renzo, M., Liu, J., Kammoun, A., and Alouini, M.-S. (2020). Beamforming through reconfigurable intelligent surfaces in single-user MIMO systems: SNR distribution and scaling laws in the presence of channel fading and phase noise. *IEEE Wirel. Commun. Lett.* 10, 77–81. doi:10.1109/lwc.2020.3021058
- Rostami Ghadi, F., Wong, K.-K., New, W. K., Xu, H., Murch, R., and Zhang, Y. (2024). On performance of RIS-aided fluid antenna systems. *IEEE Wirel. Commun. Lett.* 13 (8), 2175–2179. doi:10.1109/lwc.2024.3405636
- Shaikh, M. H. N., Bohara, V. A., Srivastava, A., and Ghatak, G. (2022). "On the performance of RIS-Aided NOMA system with non-ideal transceiver over Nakagami- m

Conflict of interest

The author(s) declared that this work was conducted in the absence of any commercial or financial relationships that could be construed as a potential conflict of interest.

Generative AI statement

The author(s) declared that generative AI was not used in the creation of this manuscript.

Any alternative text (alt text) provided alongside figures in this article has been generated by Frontiers with the support of artificial intelligence and reasonable efforts have been made to ensure accuracy, including review by the authors wherever possible. If you identify any issues, please contact us.

Publisher's note

All claims expressed in this article are solely those of the authors and do not necessarily represent those of their affiliated organizations, or those of the publisher, the editors and the reviewers. Any product that may be evaluated in this article, or claim that may be made by its manufacturer, is not guaranteed or endorsed by the publisher.

fading," in 2022 IEEE Wireless Communications and Networking Conference (WCNC) (IEEE), 1737–1742.

Shaikh, M. H. N., Rabie, K. M., Elganimi, T. Y., Li, X., Hashmi, M. S., and Nauryzbayev, G. (2025). Multi-STAR-RISNOMA: clustering, RIS assignment and power optimization. *IEEE Trans. Veh. Technol.* 74 (4), 6389–6405. doi:10.1109/tvt.2024.3509518

Statista Research Department (2023). Number of IoT-connected devices worldwide from 2019 to 2030 (in billions). Available online at: <https://www.statista.com/statistics/1183457/iot-connected-devices-worldwide/>.

Tlebaldiyeva, L., Nauryzbayev, G., Arzykulov, S., and Eltawil, A. M. (2021). Performance of NOMA-Based mmwave D2D networks under practical system conditions. *IEEE Access* 9, 958–974. doi:10.1109/access.2021.3132084

Tlebaldiyeva, L., Nauryzbayev, G., Arzykulov, S., Eltawil, A., and Tsiftsis, T. (2022). "Enhancing QoS through fluid antenna systems over correlated Nakagami- m fading channels," in 2022 IEEE Wireless Communications and Networking Conference (WCNC), 78–83.

Tlebaldiyeva, L., Arzykulov, S., Dadlani, A., Rabie, K. M., and Nauryzbayev, G. (2023). "Exploring the performance of fluid antenna system (FAS)-Aided B5G mmWave networks," in GLOBECOM 2023 - 2023 IEEE Global Communications Conference, 7568–7573.

Tlebaldiyeva, L., Arzykulov, S., Tsiftsis, T. A., and Nauryzbayev, G. (2024). Exploiting FAS for cooperative NOMA-based full-duplex mmWave networks with imperfections. *Ad Hoc Netw.* 155, 103400. doi:10.1016/j.adhoc.2024.103400

Trigui, I., Ajib, W., and Zhu, W.-P. (2020). A comprehensive study of reconfigurable intelligent surfaces in generalized fading. *arXiv Preprint arXiv:2004.02922*.

Vu, T.-H., Pham, Q.-V., Nguyen, T.-T., da Costa, D. B., and Kim, S. (2024a). Enhancing RIS-aided two-way full-duplex communication with non-orthogonal multiple access. *IEEE Internet Things J.* 11 (11), 19963–19977. doi:10.1109/JIOT.2024.3368224

Vu, T.-H., Pham, Q.-V., Nguyen, T.-T., Costa, D. B. d., and Kim, S. (2024b). Enhancing RIS-aided two-way full-duplex communication with nonorthogonal multiple access. *IEEE Internet Things J.* 11 (11), 963–977. doi:10.1109/jiot.2024.3368224

Wang, M., Liu, Z., and Dong, J. (2022). Liquid metal-embedded layered-PDMS antenna for flexible and conformal applications. *Front. Phys.* 10, 872992. doi:10.3389/fphy.2022.872992

Wang, T., Badiu, M.-A., Chen, G., and Coon, J. P. (2022). Outage probability analysis of STAR-RIS assisted NOMA network with correlated channels. *IEEE Commun. Lett.* 26 (8), 1774–1778. doi:10.1109/lcomm.2022.3174453

- Wang, R., Zheng, P., Kotte, V. V., Rauf, S., Yang, Y., Rahman, M. M. U., et al. (2025). Electromagnetically reconfigurable fluid antenna system for wireless communications: design, modeling, algorithm, fabrication, and experiment. *IEEE J. Sel. Areas Commun.*, 1. doi:10.1109/jsac.2025.3625163
- Wong, K., Tong, K., Chen, Y., and Zhang, Y. (2022). Closed-form expressions for spatial correlation parameters for performance analysis of fluid antenna systems. *Electron. Lett.* 58 (11), 454–457. doi:10.1049/ell2.12487
- Yao, J., Lai, X., Zhi, K., Wu, T., Jin, M., Pan, C., et al. (2026). “A framework of FAS-RIS systems: performance analysis and throughput optimization,” in *IEEE Transactions on Wireless Communications*. 25. 1333–1348. doi:10.1109/TWC.2025.3590458
- Yao, J., Zheng, J., Wu, T., Jin, M., Yuen, C., Wong, K.-K., et al. (2025). “FAS-RIS communication: model, analysis, and optimization,” in *IEEE Transactions on Vehicular Technology*. 74 (6), 9938–9943. doi:10.1109/TVT.2025.3537294
- Zhakupov, Z., Rabie, K. M., Li, X., and Naurzybayev, G. (2023). Accurate approximation to channel distributions of cascaded RIS-aided systems with phase errors over Nakagami- m channels. *IEEE Wirel. Commun. Lett.* 12 (5), 922–926. doi:10.1109/lwc.2023.3251647